Hierarchical multiscale modeling of polymer-solid interfaces: atomistic to coarse-grained description, and structural and conformational properties of polystyrene-gold systems.

Karen Johnston*,† and Vagelis Harmandaris*,‡,¶

Max Planck Institute for Polymer Research, Ackermannweg 10, 55128 Mainz, Germany, and Department of Applied Mathematics, University of Crete, GR-71409 Heraklion, Crete, Greece

E-mail: johnston@mpip-mainz.mpg.de; vagelis@tem.uoc.gr

Supporting Information

Mapping schemes

We note here that for technical reasons the beads for the surface interaction are not identical to the beads in the CG model. In the CG model, the C backbone atom that is attached to the phenylene group and its H atom, are shared between neighboring E beads. For the PMF calculations the bead centers correspond to the center of mass of the group of atoms contained within an ethylene or phenylene subunit, as shown in Figure 1, since it is not possible to separate forces between shared

*To whom correspondence should be addressed
†Max Planck Institute for Polymer Research, Ackermannweg 10, 55128 Mainz, Germany
‡Department of Applied Mathematics, University of Crete, GR-71409 Heraklion, Crete, Greece
¶IACM FORTH, GR-71110 Heraklion, Crete, Greece

atoms. This difference in the backbone bead centers of mass is not expected to influence the results significantly and the behavior of the CG system has been carefully compared to the AA systems.

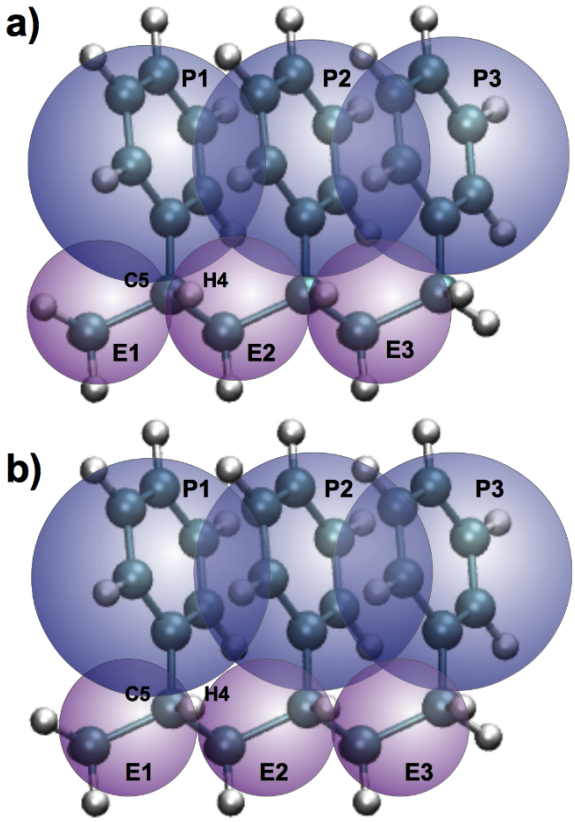

Figure 1: CG bead labelling for a) CG bulk interactions and b) surface interaction of a PS isotactic trimer. Atoms C5 and H4 in the picture are shared between beads E1 and E2 in the CG bulk model but belong to E1 in the surface interaction.

Spherical approximation

For the S5 10mer films there was an extra peak in the CG films that did not appear in the AA film. This extra peak was shown to be due to the P2 beads (central phenylene groups). There was a small difference between the PMF for the central P bead on going from a 3mer to 5mer to 7mer oligomer. To check whether this second peak was a result of long range correlations that are neglected by using the 3mer to generate the PMF we calculated the density profiles for a film of 100 3mers between gold surfaces. The films were approximately 3 nm thick and the density profiles are shown in Figure 2. It can be seen that the profiles for the P2 beads in the CG systems exhibit only

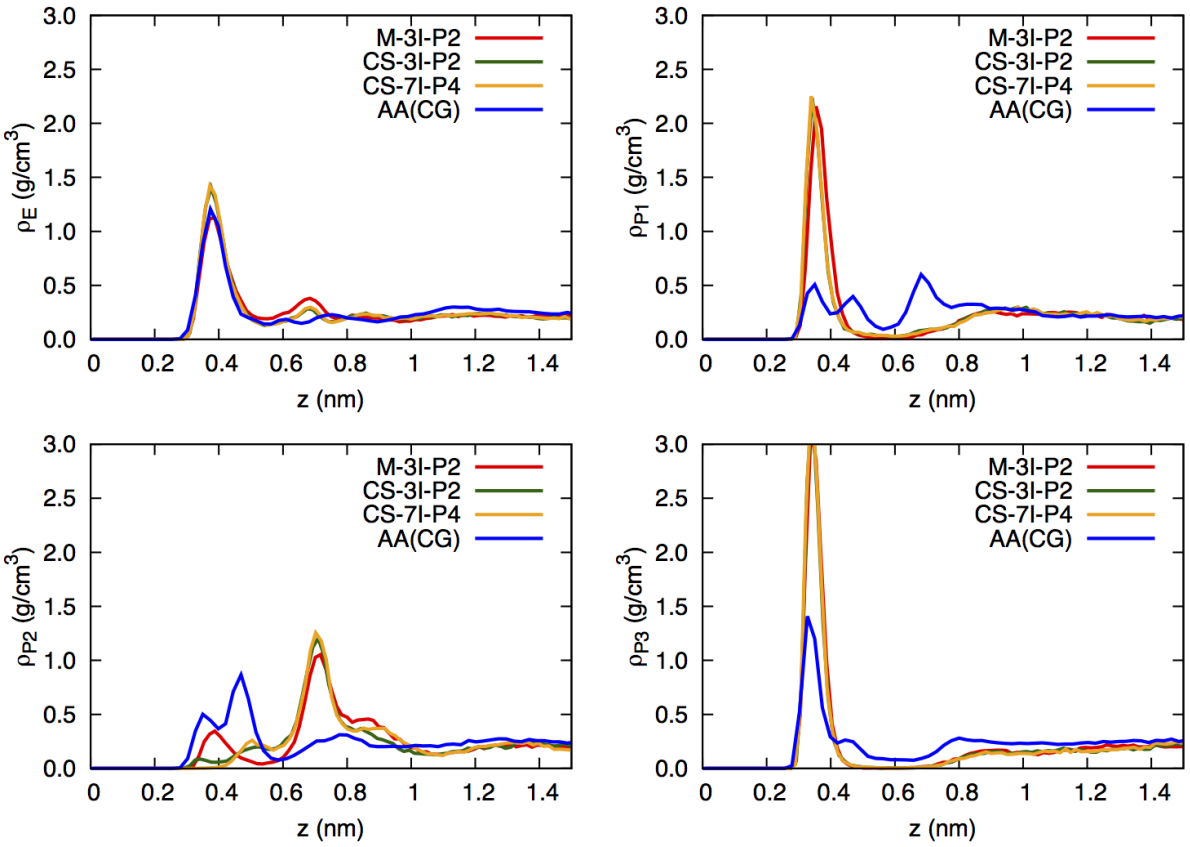

Figure 2: Bead density profiles for an 3 nm film of 100 trimers for a) ethylene beads, b) P1 beads, c) P2 beads and d) P3 beads.

a small peak(s) around 0.3-0.5 nm and a large peak at around 0.7 nm from the surface. This does not correspond to the AA film, which has a large double peak at around 0.3-0.5 nm and only a very small feature around 0.8 nm. There are similar differences in the P1 density profiles, although in this case the CG models predict a large peak around 0.4 nm compared to the AA results. However, the three CG potentials are in reasonable agreement with each other and we conclude that the difference is not due to long-range correlations in the polymer chain but is due to the spherical approximation and possibly also small differences in the angular distributions between the AA and CG models.

Equilibration

As stated in the manuscript, equilibration of long-chain polymer melts is a tricky issue. A measure of equilibration is that the ensemble-averaged end-to-end vector has decorrelated. For long chains the decorrelation time is not reachable even in CG simulations and the sample must be annealed at high temperature and then cooled down to 500 K. We have used this technique for the 50, 100 and 200mer chains (the 10mer system decorrelated within 1 ns (CG time) at 500 K). The annealing temperatures were chosen so that the systems decorrelated within 10 ns. The annealing temperatures were 800 K for the 50 and 100mer systems and 1000 K for the 200mer system. The dependence of the properties on the cooling rate were checked by cooling at two different rates, namely 10 K ns^{-1} and 1 K ns^{-1}. The decorrelation times are shown in Figure 3. To check that the

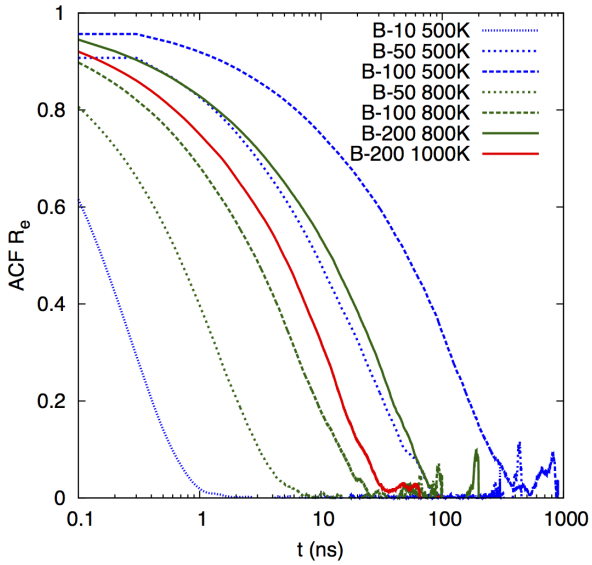

Figure 3: Decorrelation of the end-to-end vector for bulk polystyrene with different chain lengths at different temperatures.

systems are relaxed, i.e. no local strain in the polymer chains, the internal distances were analyzed. As can be seen from Figure 4, the curves for all systems are smoothly increasing up until around 50 monomers. After this there are some fluctuations in the curves, which reflects the statistical uncertainty in the end-to-end distances. The averaged data for all the films and cooling rates is given in Table 1.

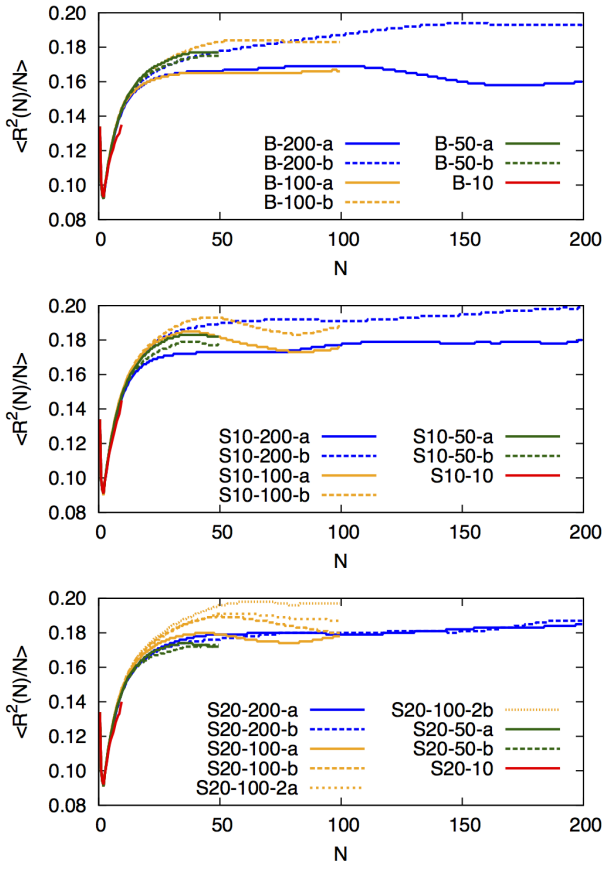

Figure 4: Internal distances for bulk systems (top), 10 nm films (middle) and 20 nm films (bottom).

Density profiles and partial densities

The density profile for the S10 films and the partial densities for the S10-10 and S10-200 films are shown in Figure 5. The profiles of the 10 nm films are indistinguishable from the 20 nm films (shown in the main manuscript). The partial densities for the 10mer and 200mer 10 nm films, shown in Figure 5(b) and (c), are very similar for the different chain lengths. Only a small difference in the density of the P beads in the first peak can be seen.

Estimate of interphase width

To estimate the width of the interphase we fitted the conformation tensor component $\mathbf{C}_{zz}(z)$ using a hyperbolic tangent of the form

$$\mathbf{C}_{zz}(z) = \tanh(z/A_{zz})$$

Table 1: Summary of the CG systems studied and their averaged properties. N_{chain} is the number of chains of N monomers. The cooling rate, Γ is in K/ns. The box lengths, L_x and $\langle L_z \rangle$, R_{e} and R_{g} are in nm and the average density ρ is in g cm^{-3}. The bulk systems are in cubic boxes with $L_x = L_z$ so only $\langle L_z \rangle$ is given. For the slabs the box is hexagonal with $L_y = \sqrt{3}L_x/2$. A is the parameter used in fitting the hyperbolic tangent to the $\mathbf{C}_{zz}$ profile, as discussed in the next section.

Label	N	N_{chain}	Γ	L_x	$\langle L_z \rangle$	$\langle \rho \rangle$	$\langle R_{\text{e}} \rangle$	$\langle R_{\text{g}} \rangle$	A_{zz}	A_{par}
B-10	10	50	-	-	4.47	0.967	1.55	0.62	-	-
S20-10	10	200	-	4.616	19.34	0.969	1.58	0.62	0.854	0.683
S10-10	10	100	-	4.616	9.64	0.972	1.61	0.62	1.021	0.862
S5-10	10	50	-	4.616	4.79	0.978	1.65	0.63	-	-
B-50-a	50	50	10	-	7.50	1.025	3.91	1.63	-	-
B-50-b	50	50	1	-	7.50	1.025	3.89	1.62	-	-
S20-50-a	50	100	10	6.347	24.18	1.025	3.86	1.63	0.974	0.207
S20-50-b	50	100	1	6.347	24.19	1.025	3.86	1.62	0.935	0.020
S10-50-a	50	50	10	6.347	12.10	1.024	3.92	1.65	0.998	0.544
S10-50-b	50	50	1	6.347	12.10	1.024	3.92	1.64	0.926	0.390
B-100-a	100	50	10	-	9.42	1.033	5.35	2.28	-	-
B-100-b	100	50	1	-	9.42	1.033	5.61	2.38	-	-
S20-100-a	100	100	10	9.232	22.70	1.032	5.51	2.36	0.899	0.559
S20-100-b	100	100	1	9.232	22.70	1.032	5.57	2.40	1.218	0.553
S20-100-2a	100	100	10	9.232	22.70	1.032	5.64	2.41	1.129	0.296
S20-100-2b	100	100	1	9.232	22.70	1.032	5.81	2.45	1.207	0.761
S10-100-a	100	50	10	9.232	11.37	1.031	5.49	2.38	1.170	0.617
S10-100-b	100	50	1	9.232	11.37	1.031	5.63	2.42	1.145	0.925
B-200-a	200	50	10	-	11.86	1.037	7.30	3.23	-	-
B-200-b	200	50	1	-	11.86	1.038	8.16	3.43	-	-
S20-200-a	200	100	10	12.694	23.93	1.036	8.06	3.39	0.937	0.464
S20-200-b	200	100	1	12.694	23.93	1.036	7.96	3.36	0.764	0.208
S10-200-a	200	50	10	12.694	11.99	1.033	7.73	3.29	0.989	0.401
S10-200-b	200	50	1	12.694	11.98	1.034	8.19	3.48	1.186	0.849

where A_{zz} is a fitting parameter and z is in units of R_{g}. Similarly, the $\mathbf{C}_{\text{par}}$ profiles were fit using an equation of the form

$$\mathbf{C}_{\text{par}}(z) = 1 + \exp\left[-\frac{z}{A_{\text{par}}}\right].$$

For the S10 films the functions were fit in the range 0-6 nm and for the S20 films they were fit in the range 0-12 nm. The average values for A_{zz} and A_{par} are 1.023 R_{g} and 0.521 R_{g}, respectively. The fitted values of A_{zz} and A_{par} are given in Table 1 and the functions are plotted in Figure 6b). It

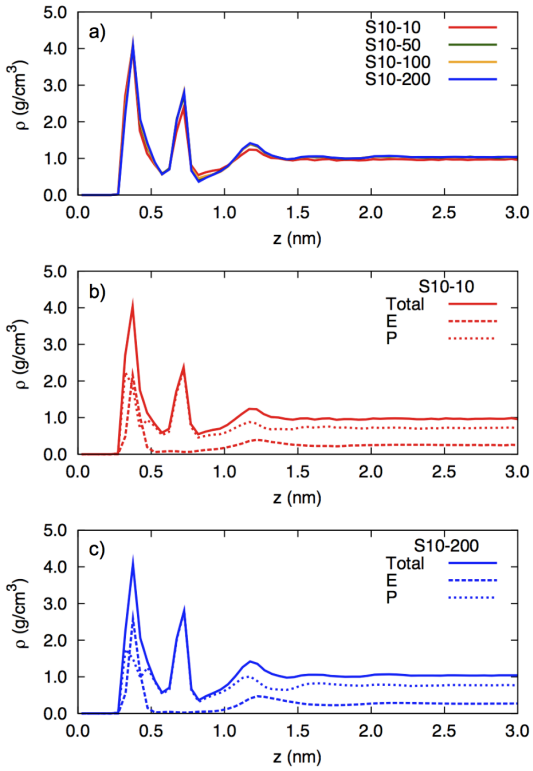

Figure 5: CG bead density profiles for the 10 nm films are shown in a). Partial bead densities, showing the bead P and E contributions, are shown for b) the S10-10 film and c) the S10-200 film.

is clear from the figure that the data for $\mathbf{C}_{\text{par}}$ is noisier than for $\mathbf{C}_{zz}$. Figure 6a) shows the $\mathbf{C}_{\text{par}}$ data for films listed in the main manuscript.

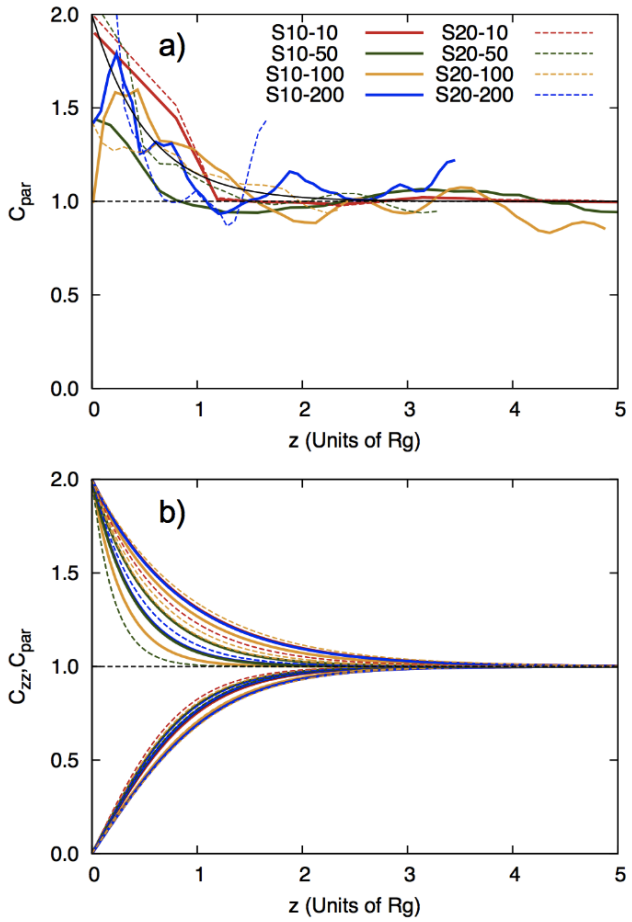

Figure 6: a) The conformation tensor profiles for $\mathbf{C}_{\text{par}}$ and the average of all the exponential functions fitted to the data (black line). b) The fits to the exponential and hyperbolic tangent functions for $\mathbf{C}_{\text{par}}$ and $\mathbf{C}_{zz}$.